Sensors & Transducers, Vol. 25, Special Issue, December 2013, pp. 140-146

Sensors & Transducers

http://www.sensorsportal.com

Implementation of a Driver Chip for the Three-Phase DC Brushless-Motor with Hall Sensors

[*] Shen-Li Chen and [2] Hsiang-Pei Ou
Dept. of Electronic Engineering, National United University, MiaoLi City 36003, Taiwan
[*] Tel.: +886-37381525, fax: +886-37362809
[*] E-mail: jackchen@nuu.edu.tw

Received: 16 September 2013 /Accepted: 15 October 2013 /Published: 23 December 2013

Abstract: Design and analysis of a driver chip for the three-phase DC brushless-motor by using a 0.6 μm CMOS process is investigated in this paper. In the CMOS process, a lot of components, i.e., control and power circuits are integrated in the same chip. Here, we will focus on the design of high-current driver part and present the results obtained from the motor operating at different situations. Eventually, an analysis of this circuitry system, it is found that the driving current can be up to 500 mA as in the three-phase DC motor operation. Moreover, in order to improve the operation accuracy of this DC brushless-motor over the entire speed control range, this paper develops a capacitor filter by using a Xilinx IC and Hall sensors feedback. By a capacitor filter adding, experimental data show a 280 % reduction of noise peak voltage in Hall sensors output and 60 % reduction of noise peak voltage (at low level) in the OP output have been achieved at rotation speed of 2500 RPM. *Copyright © 2013 IFSA.*

Keywords: Capacitor filter, Hall sensor, Signal-to-noise ratio, Three-phase DC brushless-motor, Xilinx IC.

1. Introduction

Microminiaturized DC brushless motors are widely used in PC, NB, workstation and information appliances for DVD ROM rotation driving or air cooling due to the characteristics of simple mechanical construction, low cost, high efficiency, and maintenance free. Meanwhile, with rapidly development of semiconductor process, the integration of control and drive system of DC brushless motors has been widely implemented in a same IC. As compared with the BJT technology, the CMOS process can be achieved a high complexity at same area by using pMOS and nMOS devices to accomplish a driver chip [1-9]. The TSMC 0.6 μm CMOS process has been used to develop a high-current driving chip in this work, and the supply voltage is a 5 V bias, meanwhile, this circuit will have an 8 ohm loading. Consequently, it's driving performance and high-current heat performance is necessary to be evaluated. Finally, this chip will be worked with an inductance loading, however, when the chip rotated in a very high speed the noise problem should be careful considered. The other circuit may be influenced by the noise coupling when a mix-mode IC designed. Therefore, how to avoid the power driver cross-talk with digital and analog circuits is an urgent need.

2. Experimental Details

A block diagram of three-phase DC brushless-motor driving IC is shown in Fig. 1. And, it has three coil terminals, we define it as W, V, and U. In order to let the motor ran a suitable rotation, the electric current must execute the following phase-change-order, i.e., for each time only changing & conducting one phase shown in Tables 1 and 2.

Article number P_SI_453

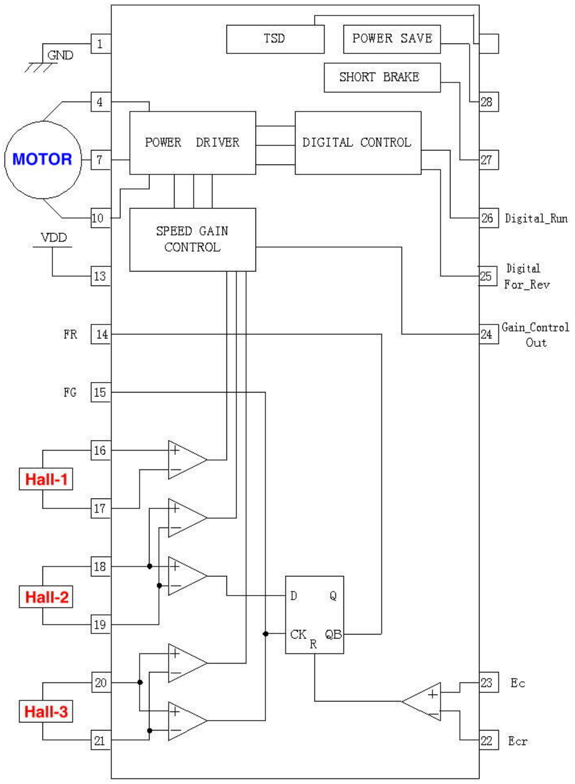

Fig. 1. Block diagram of a three-phase DC brushless-motor driving IC.

Table 1. Phase-change-order table for a three-phase DC brushless-motor.

Source	Sink
W	V
W	U
V	U
V	W
U	W
U	V

Table 2. Digital topology of Hall sensors and MOSTs conducting order.

Forward or Reverse	Hall-1	Hall -2	Hall -3	W_p	W_n	V_p	V_n	U_p	U_n	Source →Sink
Fwd	1	1	0	0	1	1	0	1	1	W→V
Fwd	1	0	0	0	1	1	1	1	0	W→U
Fwd	1	0	1	1	1	0	1	1	0	V→U
Fwd	0	0	1	1	0	0	1	1	1	V→W
Fwd	0	1	1	1	0	1	1	0	1	U→W
Fwd	0	1	0	1	1	1	0	0	1	U→V
Rev.	1	1	0	1	0	0	1	1	1	V→W
Rev.	1	0	0	1	0	1	1	0	1	U→W
Rev.	1	0	1	1	1	1	0	0	1	U→V
Rev.	0	0	1	0	1	1	0	1	1	W→V
Rev.	0	1	1	0	1	1	1	1	0	W→U
Rev.	0	1	0	1	1	0	1	1	0	V→U

Moreover, this three-phase DC brushless-motor driver will have six MOSFETs, in which it is consisted of three pMOSTs (W_p, V_p, U_p) and three nMOSTs (W_n, V_n, U_n), and each MOSFET device has being with L= 0.75 μm and W=10,000 μm geometric dimension. During the motor driver working, the pMOS is to provide the driving current, in the following step this current fed into a coil and returned to the nMOS, the nMOS is to provide the current-sink port. When the DC brushless-motor works, two MOSFETs will be turned on at the same time. The realized IC and system framework and are shown in Figs. 2 and 3.

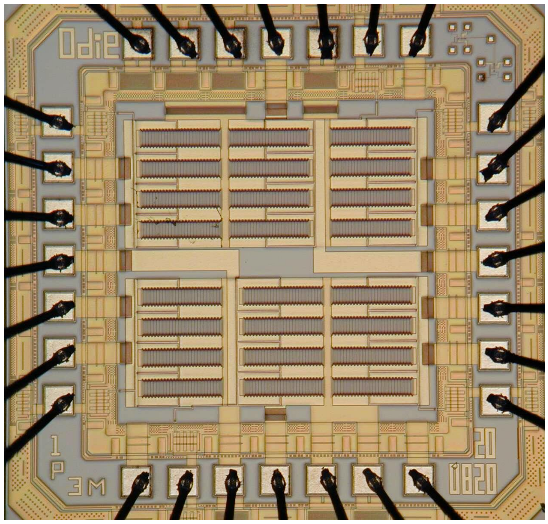

Fig. 2. Realized IC of the driver part.

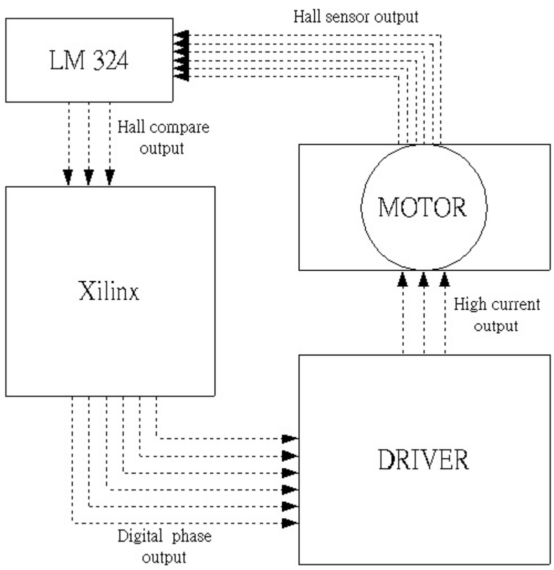

Fig. 3. Realized IC of the driver part.

As this chip driving, the heat-sink performance should be cared evaluated as a chip operated. The digital part of Fig. 1 will be emulated and used a Xilinx IC and the Hall device feeds back [10-20] by using an OP, where the Hall OP circuit and the simulation results are shown in Figs 4 and 5, respectively. A three-phase motor driver will have six

MOSFETs and the driver package is a 28 pins porcelain type. In order to measure the temperature behaviour of the driver devices, a temperature sensor is set under the driver chip. The I-V characteristics of the nMOS and pMOS are shown in Figs. 6 and 7.

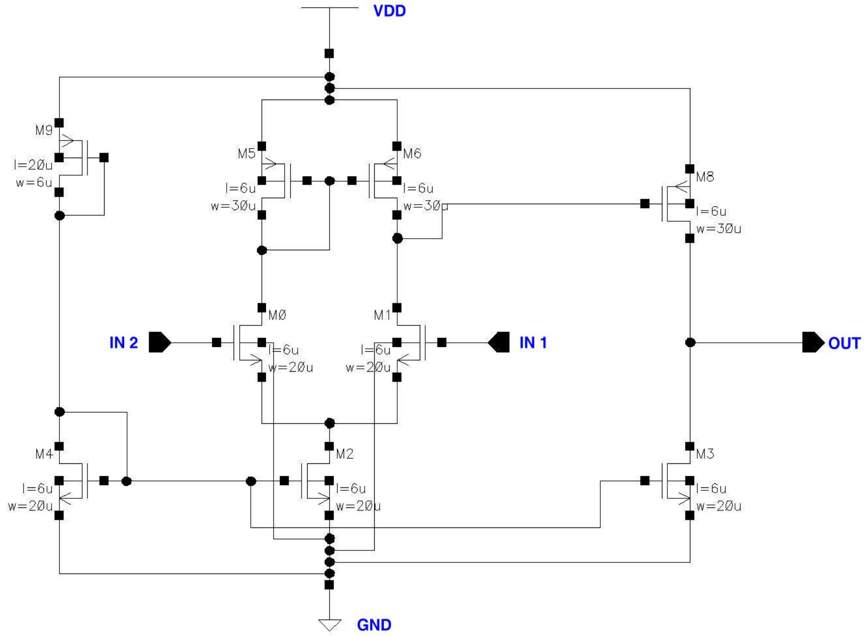

Fig. 4. Schematic circuit of a Hall OP.

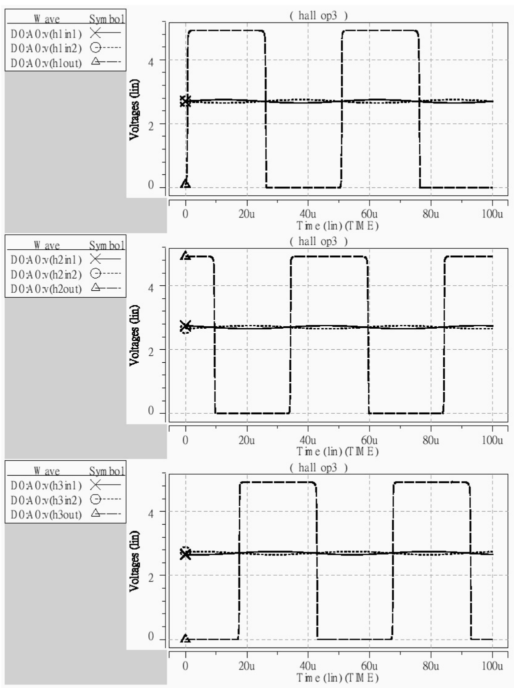

Fig. 5. Output simulation results of a three-phase Hall OP.

In the following step, we will analysis heat sink performances of the driver chip. As the device loading current being 500 mA and the temperature versus time recorded every three second, the measurement diagram was shown in Fig. 8. Eventually, the final stability temperature of this chip was reached 67.7 °C.

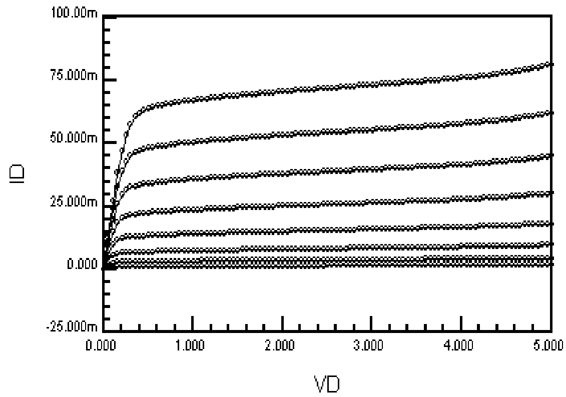

Fig. 6. The I-V characteristics of an nMOSFET in this driver.

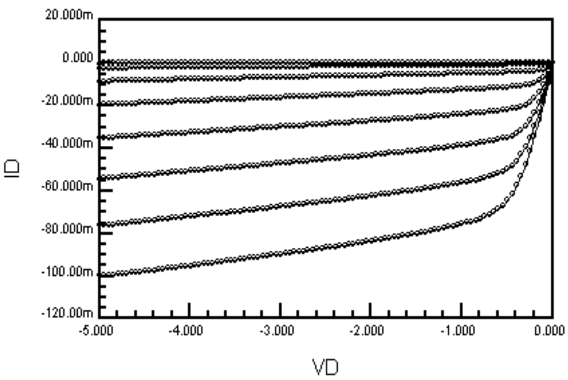

Fig. 7. The I-V characteristics of a pMOSFET in this driver.

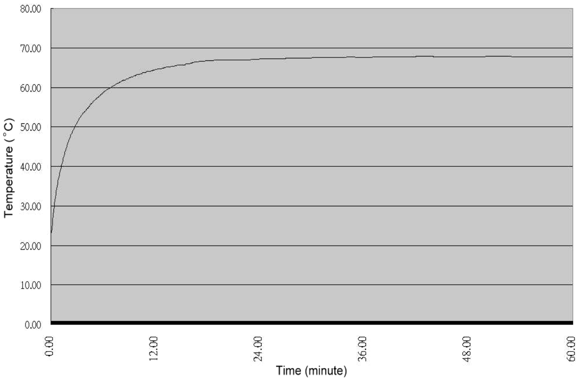

Fig. 8. Diagram of temperature vs. operation time.

In the theoretical driving-ability calculation, the driver current can be up to 450 mA as a loading is 8 ohm by using the HSpice simulator. However, in fact the motor involves an inductance loading, every phase loading is about 2.7 ohm, so we add a 3 ohm cement resistance in every phase connected point. As the waveform of chip to cement resistance and cement resistance to motor is compared, it is found that, in real measurement, the motor forward current will be with 0.18 A, meanwhile, the reverse current be with 0.41 A. Figs. 9-12 show the waveform of this driver chip driven a DC brushless-motor.

When a motor being operated, it can result in a lot of noise signals, these noises will influence the other circuits operation, so we add a capacitor filter to ground for every motor phase node. Fig. 13 shows the comparison of waveforms as removing the capacitor filter and motor operated for driver-out-node to cement resistance and cement resistance to motor node. Similarly, Fig. 14 shows that the comparison of waveforms as the capacitor filter removing and motor braked for driver-out-node to cement resistance and cement resistance to motor node. Figs. 15 and 16 show that the waveforms of Hall sensor to OP node as adding a capacitor filter and removing this filter, respectively. In the same manner, Figs. 17 and 18 show the waveforms comparison of OP output port as adding a capacitor filter and removing this filter, respectively. From Figs. 15-18, a 280 % reduction of noise peak current in Hall sensors output and 60 % reduction of RMS current (at low level) in the OP output have been achieved at rotation speed of 2500 RPM.

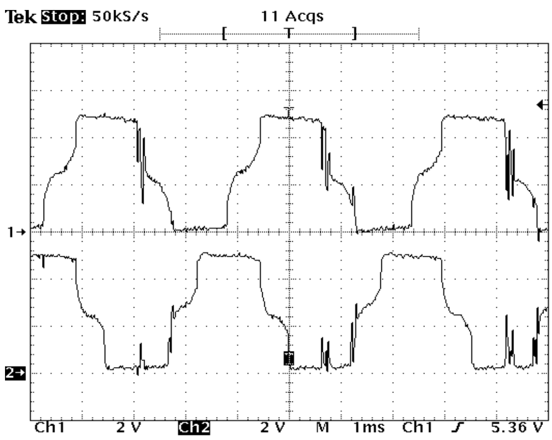

Fig. 9. The waveform of driver to resistance in any two ports.

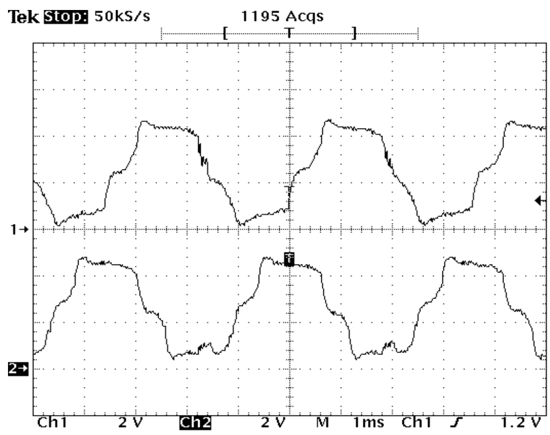

Fig. 10. The waveform of resistance to motor node in any two ports.

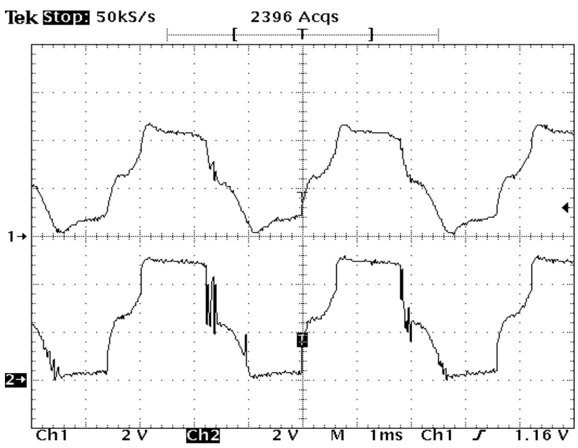

Fig. 11. The waveform comparison of driver to resistance and resistance to motor node.

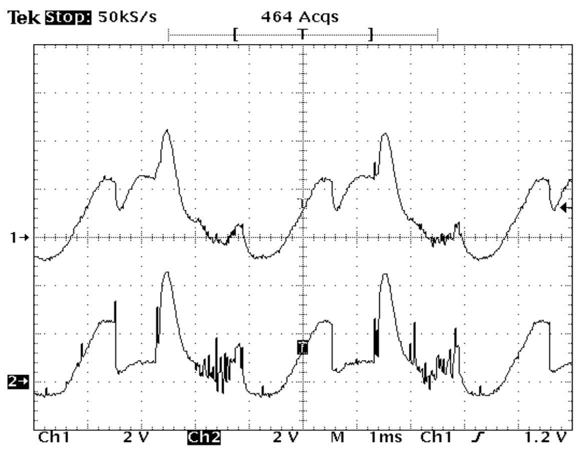

Fig. 12. The waveform comparison of driver to resistance and resistance to motor node as motor braked.

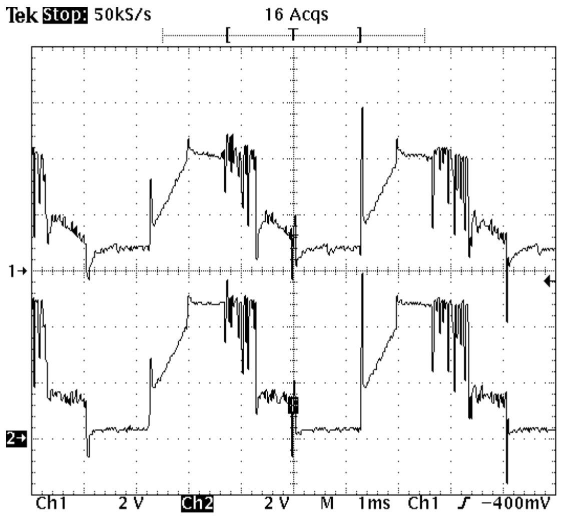

Fig. 13. Waveforms comparison of chip output-node to cement resistance and cement resistance to motor node as a capacitor filter removed and motor operated.

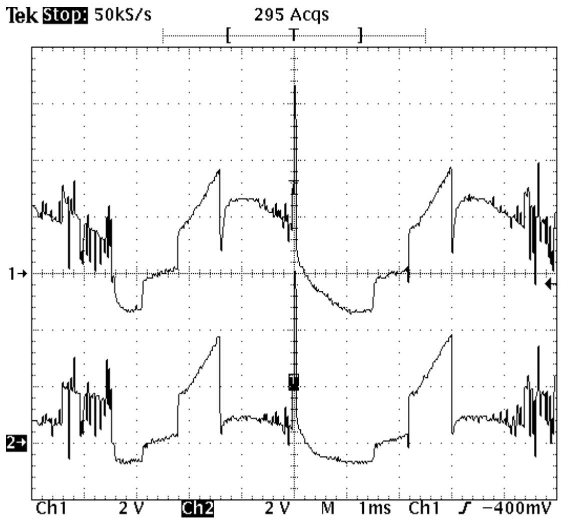

Fig. 14. Waveforms comparison of chip output-node to cement resistance and cement resistance to motor node as a capacitor filter removed and motor braked.

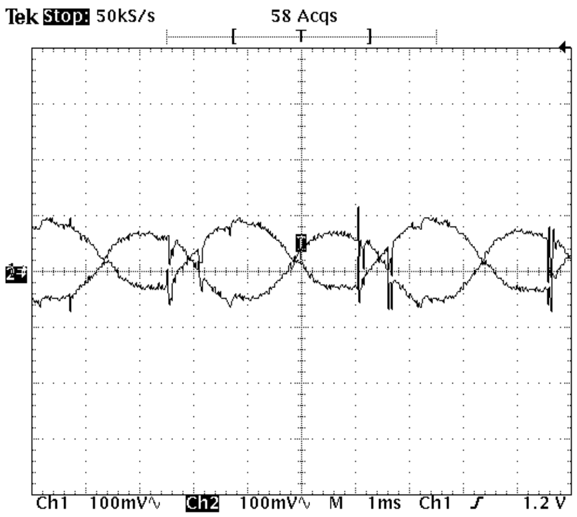

Fig. 15. Waveforms of Hall-sensor to OP as a capacitor filter added.

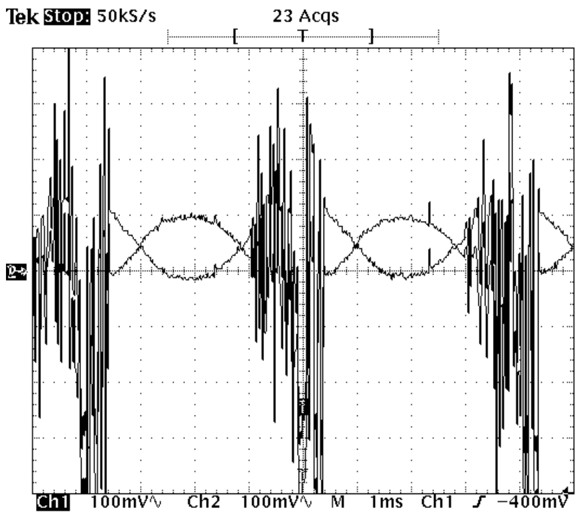

Fig. 16. Waveform of Hall-sensor to OP as a capacitor filter removed.

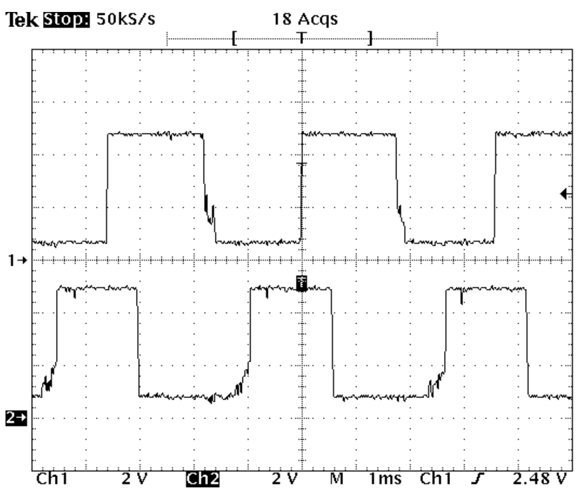

Fig. 17. Waveform of an OP output node as a capacitor filter added.

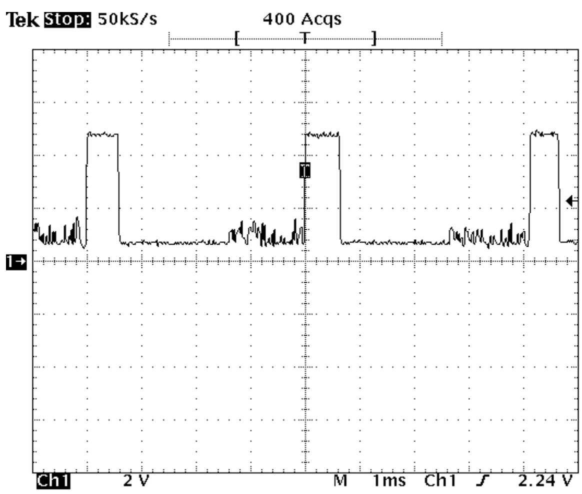

Fig. 18. Waveform of an OP output node as a capacitor filter removed.

3. Results and Discussions

Because this driver chip provides a high current driving ability, therefore, the chip temperature will be risen suddenly see Fig. 8. If the chip heat-sink ability is not so good, the chip reliability will be influenced. The package type of this driver is ceramics, the heat sink is to be competent enough if we pay attention to the temperature rising time.

Driving performance of this driver chip is very good when a long-time (1 hr) and a high-current (500 mA) conditions operated. Eventually, even current up to (900 mA), only the bonding wire was fused in this test-chip. A double guard-ring was also used in this driver chip for a high current situation, the latch-up phenomena can be avoided in these power pMOS and nMOS transistors.

As a DC brushless-motor operated in a very high rotation speed, it will create lots of noise coupling as shown in Figs. 13, 14, 16, and 18. However, if the signal-to-noise ratio is too low such that an OP can't compare the correct waveform, therefore, motor will be not correctly operated. And, the delivery current can be from 0.18 A up to 0.5 A. Why this current rose up so high, which is due to the Xilinx IC can't receive a correct signal such that its output will be not correct. In the same time was added some noise levels, therefore, this chip switched to an unknown state (the current maybe up to so high). Nevertheless, it can be conclusion that the designer must be paid much attention to the noise problems as in a three-phase DC brushless-motor driver chip design.

4. Conclusions

This work has been implemented by a 0.6 µm CMOS process for the three-phase DC brushless-motor applications. After above measurement tests, it is known that this CMOS process can be used for a high-current driver design. But, it is necessary to pay attention to some questions, such as the heat-sink influence by a chip package (the chip temperature is not suitable too high), and the power device must be obeyed the latch-up design rules especially in the high temperature situation. Nevertheless, as the power driver devices used in the switching purpose, the noise coupling and EMI issues should be avoided. How to avoid the noise problem, a capacitor filter adding in the IC application end is very important.

Acknowledgements

In this work, authors would like to thank the National Chip Implementation Center in Taiwan for providing the process information and fabrication platform.

References

[1]. R. Krenzke, Cang Ji, D. Killat. A 36-V H-bridge driver interface in a standard 0.35-µm CMOS process, in *Proceedings of the IEEE International Symposium on Circuits and Systems*, 2005, pp. 3651 -3654.

[2]. N. Ekekwe, R. Etienne-Cummings, P. Kazanzides, A configurable VLSI chip for DC motor control for compact, low-current robotic systems, *IEEE International Symposium on Circuits and Systems*, 2006, pp. 2297 -2230.

[3]. V. Marano, D. Arrigo, Novel fully integrated 65 W stepper motor driver IC, in *Proceedings of the International Symposium on Power Electronics, Electrical Drives, Automation and Motion*, 2006, pp. 680 -684.

[4]. Tzuen-Lih Chern, Li-Hsiang Liu, Chin-Wen Tien, DSP-based brushless DC motor sensorless drivers with sine PWM, in *Proceedings of the International Conference on Power Electronics and Drive Systems*, 2009, pp. 1349 -1353.

[5]. Wang Xitai, Zhang Xuexiu, Li Lifeng, Liu Bingshan, Brushless DC Motor Speed Control System of the Walking Aids Machine, in *Proceedings of the 2nd International Conference on Intelligent Networks and Intelligent Systems*, 2009, pp. 589 -592.

[6]. Jae-Hun Joo, Dong-Hyun Kim, Dong-Seok Sim, Jung-Keyng Choi, Design of a DSP controller and driver for the power-by-wire driving system with BLDC servo motor pump, in *Proceedings of the 8th International Conference on Electrical Engineering/ Electronics, Computer, Telecommunications and Information Technology*, 2011, pp. 573 -576.

[7]. Shih-An Li, Chia-Hung Lo, Chung-Wei Weng, Yi-Hong Chen, Min-Hao Yang, Ching-Chang Wong, Design of the wheeled robot motor controller, in *Proceedings of the International Symposium on Intelligent Signal Processing and Communications Systems (ISPACS)*, 2012, pp. 250 -253.

[8]. Hongmei Yang, Hua Gua, Xin Yu, Qingqing Zhang, Design of brushless DC motor control system based on DSP, in *Proceedings of the 2nd International Conference on, Consumer Electronics, Communications and Networks (CECNet)*, 2012, pp. 3195 -3198.

[9]. Y. Xu, H.-B. Pan, S.-Z. He, L. Li, Monolithic H-bridge brushless DC vibration motordriver with a highly sensitive hall sensor in 0.18 µm complementary metal-oxide semiconductor technology, *IET Circuits, Devices & Systems*, Vol. 7, Issue 4, 2013, pp. 204 -210.

[10]. Mu Sun Woo, Yong Ho Yoon, Seung Jun Lee, Chung Yuen Won, You Young Choe, Comparison of characteristics using two Hall-ICs and one Hall-IC for 3 phase slotless PM brushless DC motor, in *Proceedings of the 30th Annual Conference of IEEE Industrial Electronics Society*, 2004, pp. 1380 -1384.

[11]. Wen-Ta Lee, Hung-Wei Lu, Yi-Zhen Liao, Shun-Tsai Feng, Yuh-Shyan Hwang, Chip Design of Three-Phase BLDC Motor Brake Driver IC, in *Proceedings of the IEEE Conference on Electron Devices and Solid-State Circuits*, 2007, pp. 497-500.

[12]. N. Samoylenko, Qiang Han, J. Jatskevich, Improving Dynamic Performance of Low-Precision Brushless DC Motors with Unbalanced Hall Sensors, in *Proceedings of the IEEE Power Engineering Society General Meeting*, 2007, pp. 1 -8.

[13]. P. Alaeinovin, S. Chiniforoosh, J. Jatskevich, Evaluating misalignment of Hall sensors in brushless DCmotors, in *Proceedings of the IEEE Canada Electric Power Conference*, 2008, pp. 1 -6.

[14]. Myung-Jin Chung, Development of in-wheel motor system using blushless DC motor of Hall sensor type,

in *Proceedings of the International Conference on Control, Automation and Systems*, 2008, pp. 1508 -1511.
[15]. P. Alaeinovin, J. Jatskevich, Hall-sensor signals filtering for improved operation of brushless DC motors, in *Proceedings of the IEEE International Symposium on Industrial Electronics (ISIE)*, 2011, pp. 613-618.
[16]. P. Alaeinovin, J. Jatskevich, Filtering of Hall-Sensor Signals for Improved Operation of Brushless DC Motors, *IEEE Transactions on Energy Conversion*, 2012, pp. 547 -549.
[17]. Do-Yun Kim, Jung-Hyo Lee, Taeck-kie Lee, Chung-Yuen Won, Phase current sensing method using three shunt resistor for AC motor drive, in *Proceedings of the IEEE Vehicle Power and Propulsion Conference (VPPC)*, 2012, pp. 78-82.
[18]. Yun She, Output Feedback Control of Electronic Throttle Valve, *Journal of Mechatronics*, Vol. 1, No. 1, 2012, pp. 3-11.
[19]. Irfan Ullah, Qurban Ullah, Furqan Ullah, and Seoyong Shin, Sensor-Based Autonomous Robot Navigation with Distance Control, *Journal of Computational Intelligence and Electronic Systems*, Vol. 1, No. 2, 2012, pp. 161-168.
[20]. Si Young Yun, Ho Joon Lee, Jung Ho Han, Ju Lee, Position Control of Low Cost Brushless DC Motor Using Hall Sensor, in *Proceedings of the Sixth International Conference on Electromagnetic Field Problems and Applications (ICEF)*, 2012, pp. 1-4.